Groundwater

Impacts of Seawater Rise on Seawater Intrusion in the Nile Delta Aquifer, Egypt

by Ahmed Sefelnasr[1] and Mohsen Sherif[2]

Abstract

Several investigations have recently considered the possible impacts of climate change and seawater level rise on seawater intrusion in coastal aquifers. All have revealed the severity of the problem and the significance of the landward movement of the dispersion zone under the condition of seawater level rise. Most of the studies did not consider the possible effects of the seawater rise on the inland movement of the shoreline and the associate changes in the boundary conditions at the seaside and the domain geometry. Such effects become more evident in flat, low land, coastal alluvial plans where large areas might be submerged with seawater under a relatively small increase in the seawater level. None of the studies combined the effect of increased groundwater pumping, due to the possible decline in precipitation and shortage in surface water resources, with the expected landward shift of the shore line. In this article, the possible effects of seawater level rise in the Mediterranean Sea on the seawater intrusion problem in the Nile Delta Aquifer are investigated using FEFLOW. The simulations are conducted in horizontal view while considering the effect of the shoreline landward shift using digital elevation models. In addition to the basic run (current conditions), six different scenarios are considered. Scenarios one, two, and three assume a 0.5 m seawater rise while the total pumping is reduced by 50%, maintained as per the current conditions and doubled, respectively. Scenarios four, five, and six assume a 1.0 m seawater rise and the total pumping is changed as in the first three scenarios. The shoreline is moved to account for the seawater rise and hence the study domain and the seaside boundary are modified accordingly. It is concluded that, large areas in the coastal zone of the Nile Delta will be submerged by seawater and the coast line will shift landward by several kilometers in the eastern and western sides of the Delta. Scenario six represents the worst case under which the volume of freshwater will be reduced to about 513 km^3 (billion m^3).

Introduction

Groundwater represents the main source of freshwater in many countries around the globe. This is typically true in arid and semi-arid regions, where rainfall is scarce, random and insignificant and surface water bodies are limited and sometimes absent. Because of the high population density near shorelines and the tendency of people to live in, and develop the, coastal regions, coastal aquifers are generally exposed to extensive groundwater pumping which, in most cases, exceeds natural replenishment rates.

Seawater intrusion in coastal aquifers is a common problem and is encountered, with different degrees, in almost all coastal aquifers. It is regarded as a natural process that might be accelerated or retarded by external factors such as increase or decrease in the groundwater pumping, irrigation and recharge practices, land use,

and possible seawater rise due to the impacts of global warming.

The seawater intrusion problem has been under investigation for well over a century (Werner and Simmons 2009; Post and Abarca 2010). A comprehensive review on different aspects of seawater intrusion assessment, monitoring, and modeling is provided by Bear et al. (1999).

The Intergovernmental Panel of Climate Change estimated that the global mean seawater levels have risen by 10 to 20 cm during the last century. It is also estimated that during this century the seawater level rise will be in the range of 11 to 88 cm (IPCC 2001, 2007). The increase in the seawater level, due to climate change, will have major impacts on groundwater resources in coastal aquifers. First, the shoreline will shift to a new landward position and depending on the land topography this shift might be significant and the groundwater in the affected zone will become completely saline. Second, the increase in the seawater level would cause additional pressure head at the seaside and, hence, the seawater water would advance more inland. Third, climate change may cause variations in rainfall which would affect the natural replenishment of groundwater. Fourth, due to the anticipated reduction in rainfall and surface water resources in arid and semi-arid regions, the reliance on,

[1] Geology Department, Faculty of Science, Assiut University, 71516 Assuit, Egypt; ahmed.sefelnasr@yahoo.com
[2] Corresponding author: Department of Civil and Environmental Engineering, College of Engineering, United Arab Emirates University, P.O. Box # 15551, Al Ain, United Arab Emirates; (971) 3 7621694; msherif@uaeu.ac.ae

and exploration of, groundwater resources would increase to substitute for the scarcity of surface water resources and meet the water demands of the various sectors.

Sherif and Singh (1999) reported that the hydraulic gradient of the water table and/or piezometric head in the Nile Delta Aquifer would decrease due to the expected seawater rise. They also reported that deep coastal aquifers with mild hydraulic gradients would be more vulnerable under the conditions of climate change and seawater rise. For the case of the Nile Delta Aquifer, they concluded that a 0.5 m rise in the seawater level in the Mediterranean Sea would cause equiconcentration lines 35, 5, and 1 g/L to move inland by distances of 1.5, 4.5, and 9 km, respectively, under the steady state conditions. Lower equiconcentration lines were hence reported to be more sensitive to seawater level rise. Using the Sharp interface approach, Werner and Simmons (2009) concluded that their analysis of the effect of seawater intrusion under global warming conditions is in agreement with the results of Sherif and Singh (1999). An inland toe migration in the order of 5 km was achieved in the two studies for a 0.5 m sea-level rise.

Langevin and Dausman (2005) evaluated the interface movement in response to sea level rise based on the generalized characteristics of the highly permeable Biscayne Aquifer of Broward County, Florida. The seawater intrusion was investigated under three cases of variable annual rates (0.9, 4.8, and 8.8 mm/year) of sea-level rise. The freshwater isochlor line (250 mg/L) moved inland by distance of 40 m, 740 m and 1800 m, respectively, for the three cases over a simulation period of 100 years. The last scenario represented the worst scenario of an anticipated seawater level rise by 88 cm during this century (IPCC 2001).

Yechieli et al. (2010) studied the response of the Mediterranean and Dead Sea coastal aquifers to sea level variations. A fast response was observed in the Dead Sea coastal aquifer, exhibited both in the drop of the water levels and the location of the fresh-saline water interface. The simulations of the Mediterranean aquifer indicated that for the case of a steep coastal topography, simulated as a cliff, the shoreline, and the interface are not expected to shift inland. A considerable inland shift of the shoreline and the interface is expected for the flat coastal topography. They also concluded that reduced recharge due to climate change and/or overexploitation of the groundwater would enhance the shift of the interface.

Scope of Research, Method, and Assumptions

Many coastal lands in the different parts of the world are of low altitude and flat in nature. Such coastal areas are vulnerable to submergence under the condition of seawater rise. Compared to other countries, the potential impacts of seawater level rise have been little studied at the national and subnational level in Africa (Brown et al. 2011). Previous studies on the effect of possible seawater rise, due to climate change, on the Nile Delta Aquifer were mostly conducted in the vertical view and without

consideration of the significant landward shift of the shore boundary. Available studies dealt with the vertical section in the middle of the Nile Delta and no work considered the western and eastern areas (Sherif and Singh 1999).

Unlike previous studies, this article considers the landside shift of the shore boundary due to the possible rise of the water level in the Mediterranean Sea. The problem is also investigated under different scenarios of groundwater pumping. The simulations are conducted in the horizontal view to provide a better understanding for the movement of the transition zone in the entire aquifer and not only at a specific sections. The available sustainable volumes of fresh, brackish, and saline waters are assessed under different conditions. In addition to the basic run (current conditions), six other scenarios are considered. In the first three scenarios, the seawater level is assumed to rise by 0.5 m and the pumping rate was varied. Scenarios four, five, and six assume a 1.0 m seawater rise and the pumping rates were varied as in the first three scenarios. This research provides an accurate assessment for the coastal areas that would be submerged by seawater under the conditions of 0.5 and 1.0 m seawater level rise.

Sherif et al. (2012) calibrated a two-dimensional horizontal model, using FEFLOW (Diersch 2002, 2006), to simulate the seawater intrusion in the Nile Delta Aquifer at various levels below mean seawater level (0.0, 100, 200, 300, and 400 m) and deduced the dispersion zone in three different vertical cross sections. The same model is utilized in this research but with an entirely different objective and assumptions.

Few assumptions have been implemented in this work. First, the transitional processes of the climate changes are not considered. In other words, the seaside boundary is shifted landward without consideration of the lengthy time (in the order of a century) that might be required for this boundary shift under the expected gradual seawater level rise which could be in the range of 1.0 to 1.4 m by the year 2100 (Cayan et al. 2009). Second, the annual groundwater recharge from rainfall would not change under the conditions of climate change. This assumption is supported by the fact that the groundwater recharge in the Nile Delta Aquifer is mostly encountered from the Nile River, the intensive irrigation and drainage networks, and irrigation of the vast cultivated lands. Third, the water levels in the Nile River and its irrigation networks are fixed and fully controlled by the High Aswan Dam and other massive water structures. Finally, anthropogenic factors such as changes in vegetation, reduction of sediments and wadis' flow and possible changes in water diversions are not considered.

The Nile Delta Aquifer

The Nile Delta, along with its fringes, occupies an area of about 23,284 km^2. It lies between latitudes 30°05′ and 31°30′ N and longitudes 29°50′ and 32°15′E. At a distance of about 20 km North West of Cairo and at an elevation of 17 m above mean sea level, the Nile Valley

Figure 1. The Nile Delta Aquifer and its boundary conditions.

begins to open out into triangular alluvial Delta with its base (245 km) at the Mediterranean Sea. The length of the right Nile branch (Damietta) is about 240 km and that of the left branch (Rosetta) is about 235 km, Figure 1. The Nile Delta Aquifer underlies about 3.0 million acres of fertile lands. It fills a vast underground bowl situated between Cairo and the Mediterranean Sea and is considered among the largest groundwater reservoirs in the world. Several investigations in the last three decades have confirmed that seawater intrusion has migrated inland, at some locations, to a distance of more than 100 km from the Mediterranean coast, measured along the bottom boundary of the aquifer (Sherif et al. 1988; Sherif 1999).

The major portion of the annual recharge of the Nile Delta Aquifer is derived from the direct seepage from the Nile River and the extensive network of irrigation canals, as well as from infiltration of excess irrigation water. The annual overall groundwater recharge to the aquifer is estimated at 6.70 km^3/year (Kashef 1983; Mikhailova 2001).

The ground surface elevation in the Nile Delta area lies above the mean sea level except in some locations in the northern part where depressions are encountered. Field observations indicated that the major alluvial aquifer (south of Tanta), Figure 1, is generally of good groundwater quality, with salinity values of less than 1000 ppm. The salinity increases toward the north due to the effect of seawater intrusion from the Mediterranean Sea. In the northern Delta, the salinity ranges from 5000 ppm to 35,000 ppm. On the other hand,

due to the density effects, the salinity of the groundwater increases with the depth below the mean seawater level (Sherif et al. 2012).

Geological Setting

The geology of the Nile Delta basin has been extensively discussed by a number of researchers over several decades (Hurst 1952; Said 1962, 1993; Kashef 1981a, 1981b). The thickness of the Nile Delta Aquifer increases from about 200 meters in the south, near Cairo, to more than 900 m at the Mediterranean Sea. The base is a clay aquiclude with an average slope of about 4 m/km.

The strata of hydrological importance belong to the Quaternary and constitute the main water-bearing formations. These strata are composed of sands and gravels (Pleistocene and Holocene) containing few lenses of clays. These deposits are classified into Bilqas formation in the upper parts and Mit Ghamr formation in the lower parts (Coutellier and Stanley 1987). The Bilqas formation consists of clay and silt including some sand tracks and sand dunes in the coastal area. In the southern part, the Bilqas formation is thin and coarse; its thickness ranges between 5 and 25 m and it acts as an aquitard. In the northern parts, it becomes thick and fine and its thickness reaches more than 50 m; therefore, it acts as an aquiclude (Said 1962).

Mit Ghamr formation of Pleistocene begins at Cairo to the south and spreads out in a fan-like shape toward the Mediterranean Sea. It consists of sand and gravel with occasional thin clay intercalations. Clay is observed in the north with occasional discontinuity and intercalation of sand and gravel. Alternating beds of clay and sand with gravel are encountered at different locations especially in

north and northeast parts. The thickness of the sediments ranges between 200 and 400 m in the south and from 500 to 700 m in the middle. In the north, the thickness of the sediments reaches a maximum value exceeding 950 m (Said 1993). The basal portion of the deltaic deposits rests on a thick clay section which belongs to the Neogene. This clay section acts as an aquiclude. The gravelly deposits show a thinning trend both to the east and to the west.

Hydrogeological Setting

The Nile Delta Aquifer system is classified as a leaky aquifer in the southern, northern and middle parts, and a phreatic aquifer near the western and eastern borders. On the regional scale, flow within the Pleistocene Aquifer is considered essentially horizontal as the vertical flow is relatively insignificant except in the vicinity of seaside. This assumption of horizontal flow within the Pleistocene Aquifer is supported by the fact that the dimensions of the aquifer in the horizontal view are more than 100 times the depth at any point. The aquifer thickness is very small as compared to its horizontal extension. Within the clay cap, however, the flow is essentially vertical and the horizontal flow in the clay cap is negligible.

Due to the direct hydraulic contact between the Nile River and the underlying aquifer, and prior to the completion of the High Aswan dam in 1964, the potentiometric levels in the Nile Delta Aquifer were fluctuating in response to the stage of the Nile River and flood events. Upon the completion of the High Aswan dam, the flow through the Nile River was controlled and water flooding in the Nile Delta was eliminated. Hence, the potentiometric levels reached a more or less a stable pattern and reached semi-steady state conditions.

The fresh water body in the Nile Delta Aquifer occupies a huge convex lens with its maximum thickness at the southern part of the Delta. The surface water network plays an important role in relation to the groundwater flow Nile River, canals and drains varies spatially based on influent and effluent conditions. At some locations the levels of surface water bodies lie below those of the aquifer making the Nile River and canals as drains.

The most permeable water-bearing strata in the Nile Delta Aquifer has been found at depths between 55 and 150 meters from land surface. Dahab (1993) elaborated that the transmissivity reaches its minimum values in the southwestern area, where it ranges between 2000 and 3000 m²/d and its maximum values in the middle and southeastern parts, where it ranges between 9000 and 15,000 m²/d. The hydraulic conductivity of the Nile Delta Aquifer is relatively high and ranges between 70 and 100 m/d. The effective porosity over the whole area ranges between 12 and 19%, and total porosity varies between 25 and 40%, which indicates that the aquifer is mainly composed of coarse sand and gravel, Sherif (1999). The storativity of the aquifer varies between 0.01 and 0.001 in the southern parts. In the southeastern and southwestern areas, the storativity ranges between 0.1 and 0.01, which indicates that the aquifer is unconfined to

semiconfined in these areas. In the northern area, the storativity ranges between 0.0005 and 0.0009, indicating confined conditions. The vertical hydraulic conductivity in the cap layer was estimated to be about 0.67 mm/d. Sherif et al. (1988) estimated the longitudinal dispersivity and the lateral dispersivity for the Nile Delta Aquifer as 100 m and 10 m, respectively. Detailed discussions related to the hydrological setting and parameters are given in Sherif (1999).

Boundary Conditions and Hydraulic Parameters

A comprehensive three-dimensional (3D) geographical information system (GIS) database including all available geometric, geological, and hydrogeological parameters of the Nile Delta Aquifer was developed. In the vertical direction, 28 layers were introduced. The developed database allows for the development of input files for numerical simulations and also for the proper visualization of information. A 3D view of the Nile Delta Aquifer and the hydraulic conductivity is presented in Figure 2. The developed database interacts with, and acts as a pre-processor for, FEFLOW.

The main aquifer is capped by a variable thickness semi previous layer with a vertical hydraulic conductivity of 0.67 mm/d. Only vertical water fluxes (downward and upward) are allowed through the upper semi pervious clay layer and the concentration gradient across this clay layer is set as zero.

The aquifer is overlaying a thick impervious aquiclude, which does not allow for water or salt exchange. The average depth to groundwater table below the land surface ranges from 0.5 m in the north to about 5 m in southeast and southwest of the study area. With reference to the mean seawater level, the elevation of the groundwater table at Cairo, Tanta, and El Mansura are 14 m, 7 m and 2 m, respectively.

The average hydraulic gradient is estimated to be about 11 cm/km in the flow direction toward the Mediterranean Sea. The hydraulic heads in the north and east boundaries were considered as zero as the domain is bounded by the Mediterranean Sea from the north and Suez Canal from the east, Figure 1. A concentration of 35,000 mg/L is used along the coastal boundary and the initial concentration of the groundwater was set to 500 mg/L.

The southern boundary along Ismailia Canal, and the west boundary at El Nubariya Canal were considered as first type spatial dependent boundary conditions at which the water table level is controlled by the water level in the canals. In addition, the two Nile branches and other canals dissecting the inner model area were considered as constant head internal boundaries. The water levels in the two Nile branches and canals are controlled by the High Aswan dam and several other water structures and hence are considered fixed.

The aerial recharge is calculated from the average precipitation of 150 mm/year along the Mediterranean coast. This average decreases rapidly southward until
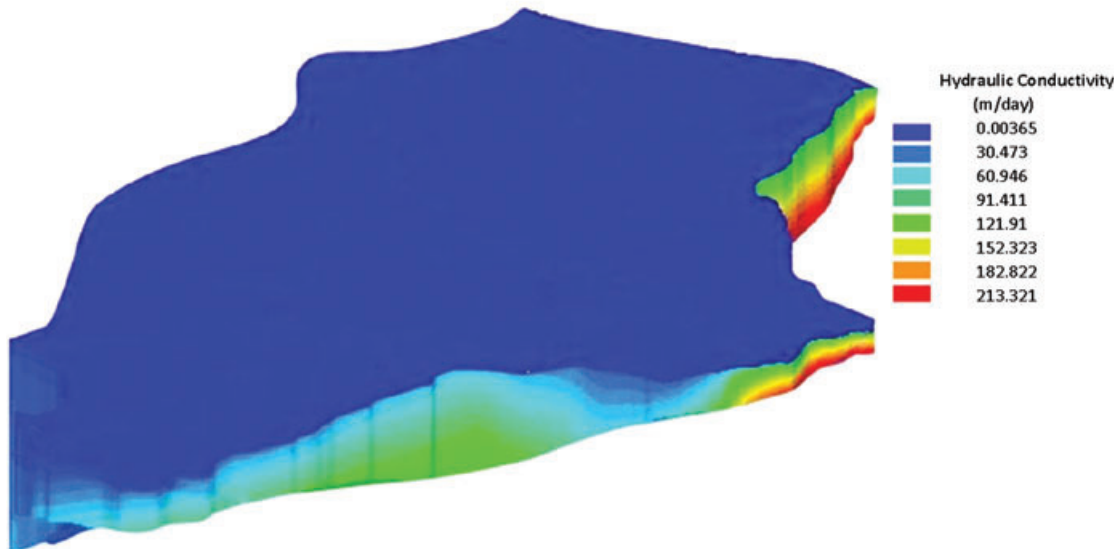
Figure 2. A three-dimensional view of the Nile Delta Aquifer.

it reaches about 26 mm/year near Cairo (Dahab 1993; El-Sadek et al. 2008). It should be noted, however, that the groundwater recharge from rainfall is relatively insignificant as the upper clay layer is very thick in the northern zone where the rainfall is appreciable and the flux through the clay layer is mostly upward. In the southern parts of the Delta, the rainfall is nominal and does not contribute tangibly to groundwater recharge. The recharge from irrigation practices is estimated as 0.54 mm/d. The average loss by evaporation is as 311 mm/year (RIGW/IWACO 1990). The overall groundwater withdrawal for all purposes is 2.3 km^3/year (2.3 billion m^3/year) (Sherif 1999; Mikhailova 2001).

Model Calibration

As discussed in Sherif et al. 2012, the time-stepping technique (Voss 1984; Diersch and Kolditz 1998) was employed to obtain a steady state solution. The model was run under transient mode with static boundary conditions. When no changes in heads and concentrations are observed over the simulation time, the steady state conditions are attained. The transient state simulation of the solute transport was carried out using automatic time step control via predictor-corrector scheme, with an initial time step of 0.001 d and a final time step of 4380 d to reach steady state conditions.

The simulation was conducted in the horizontal view and at the seawater level where the pressure is atmospheric and the equivalent freshwater head at the seaside boundary is set as zero. The calibration process involved adjustments in the hydraulic conductivities and longitudinal dispersivity coefficient using the trial an error technique, to achieve a good match with the observed groundwater levels and dispersion zone. The calibrated hydraulic conductivity of the aquifer ranged between 60 and 240 m/d.

On the basis of the laboratory experiments longitudinal dispersivities of 0.1 to 10 cm has been reported for the different types of materials. The transversal dispersivity is estimated as 10 to 20 times smaller than the longitudinal dispersivity (Klotz 1973). Longitudinal dispersivities in the field are usually much larger than those of laboratory experiments (Lenda and Zuber 1970). The main reason for this is the influence of small-scale heterogeneities in the permeability of the aquifer, which means the onset of macro dispersion. Owing to this scale behavior of dispersion, no generally valid values for longitudinal dispersion can be given (Kinzelbach 1986). Values between 0.1 and 500 m can be found in the literature (Sherif et al. 1990).

During the calibration process the ratio between the transverse to the longitudinal dispersivity coefficient was maintained at 1:10 and the longitudinal dispersivity was varied to match the concentration based on field observations. The calibrated longitudinal and transverse dispersivity coefficients were found as 70 and 7 m, respectively. The calibration process indicated that the concentration distribution and the dispersion zone are sensitive to the longitudinal and lateral dispersivities. The simulation was repeated using a higher resolution grid with 67,812 elements and 55,684 nodes (instead of 47,062 elements and 36,396 nodes) to ensure the accuracy of the solution. The same concentration distribution and dispersion zone were obtained.

The goodness-of-fit between the simulated and observed groundwater levels and concentrations was evaluated quantitatively by computing the statistics of the residuals between the simulated and observed parameters. For the groundwater levels, the calibration was conducted using 150 observation wells in different locations. Figure 3a presents the simulated and observed groundwater levels and the histogram of the frequency range of residuals. The correlation factor, R^2, between simulated
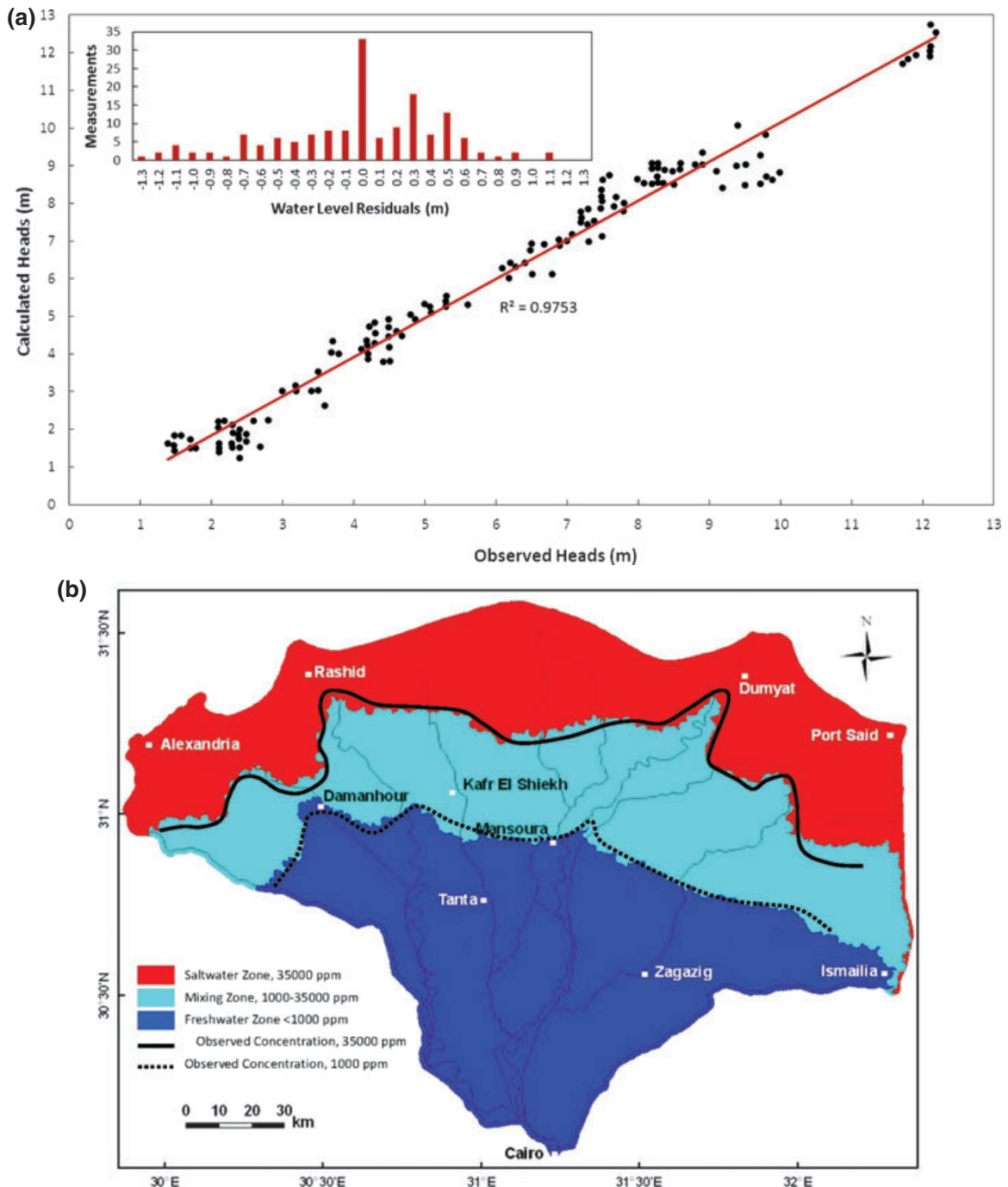
Figure 3. (a) Relationship between simulated and observed groundwater levels in 150 observation wells and the distribution of residuals. **(b)** Resulted and observed groundwater concentrations and the dispersion zone in the Nile Delta Aquifer.

and observed levels was 0.977. For the groundwater concentrations, 86 records from different observation wells were used and the same process was implemented. Table 1 presents the statistical parameters related to the calibration of groundwater levels and concentrations in the Nile Delta Aquifer. Figure 3b presents a comparison between the simulated and observed dispersion zones. The observed dispersion zone was delineated based on the field measurements of groundwater salinity. The solid and dotted lines represent the observed equiconcentration lines 35,000 and 1000 ppm; respectively.

The limited discrepancy between the calculated and observed dispersion zone might be attributed to the lack of field data in some areas and the associated interpolation to develop the observed dispersion zone. Also, it should be noted that the depths of monitoring wells from which the groundwater samples were collected and analyzed are not very much defined and may not be uniform among all monitoring wells. Since the groundwater salinity varies in the vertical direction and the depth of groundwater sampling is not defined, the observed contours of the seawater and freshwater concentrations might not be fully accurate.

Table 1
Statistical Parameters Related to the Calibration of Groundwater Levels and Concentrations in the Nile Delta Aquifer

Parameter	Groundwater Levels	Groundwater Concentration
Number of observation	150	86
Range of residuals	2.4 m	527 mg/L
Minimum residual	−1.3 m	−240 mg/L
Maximum residual	1.1 m	287 mg/L
Mean residual	−0.04 m	4.5 mg/L
Standard deviation of residuals	0.466 m	80.4 mg/L
Root mean square of residuals	0.465 m	80.05 mg/L
Standard error of residuals	0.038 m	8.67 mg/L
Skewness of residuals	−0.507 m	0.34 mg/L
Kurtosis of residuals	0.394 m	3.05 mg/L

It should also be noted that such a huge and complex groundwater system may never achieve the perfect steady state conditions. This is mostly due to the fact that, under natural conditions, the system's excitations including rainfall events, groundwater pumping, and recharge from irrigation practices will not remain constant for an extended period of time. On the basis of the comparison provided in Figure 3b, the model is considered calibrated and representative of the seawater intrusion problem in the Nile Delta Aquifer.

Results and Effects of Seawater Level Rise

Many researchers investigated seawater intrusion problems using different approaches and different models under steady and transient flow conditions (Henry 1964; Pinder and Cooper 1970; Lee and Cheng 1974; Segol and Pinder 1976; Sherif et al. 1988; Galeati et al. 1992; Simpson and Clement 2004; Kacimov and Sherif 2006; Kacimov et al. 2009; Sherif et al. 2012). Several researchers considered the effect of climate change and possible rise of seawater level on groundwater flow and seawater intrusion using both the sharp interface approach and dispersion zone approach (Oude Essink 1996; Sherif and Singh 1999; Werner and Simmons 2009; Sanford and Pope 2010; Yechieli et al. 2010). All investigations revealed the significance of climate change and the possible impacts of seawater level rise on seawater intrusion processes.

Rahmstorf et al. (2007) included more accurate seawater level measurements and concluded that the seawater level rise during the period 1993 to 2006 outpaced the IPCC projections. They elaborated that the seawater levels may be responding to climate changes and global warming more quickly than the predictions. Cayan et al. (2009) projected that, under medium to medium high emission scenarios, mean seawater level along the California coast will rise from 1.0 to 1.4 m by the year 2100. In areas where the coast erodes easily, seawater rise will likely accelerate shoreline recession.

In this study, six different scenarios were considered to simulate the possible impacts of seawater level rise and change in groundwater pumping due to possible climate change and seawater level rise. These scenarios were selected to cover the range of "actions taken to no actions taken" to reduce the impacts of climate change and groundwater pumping. The most conservative scenario, in this investigation, represents the case of 0.5 m increase in the seawater level and 50% pumping reduction. This scenario assumes that moderate seawater level rise (0.5 m) will be encountered and effective measures will also be taken to reduce the groundwater pumping. The other extreme scenario represents the case of 1.0 m seawater level rise and a 200% increase in groundwater pumping. Table 2 provides a summary of the six different scenarios. All other hydraulic parameters remained unchanged as in the base scenario.
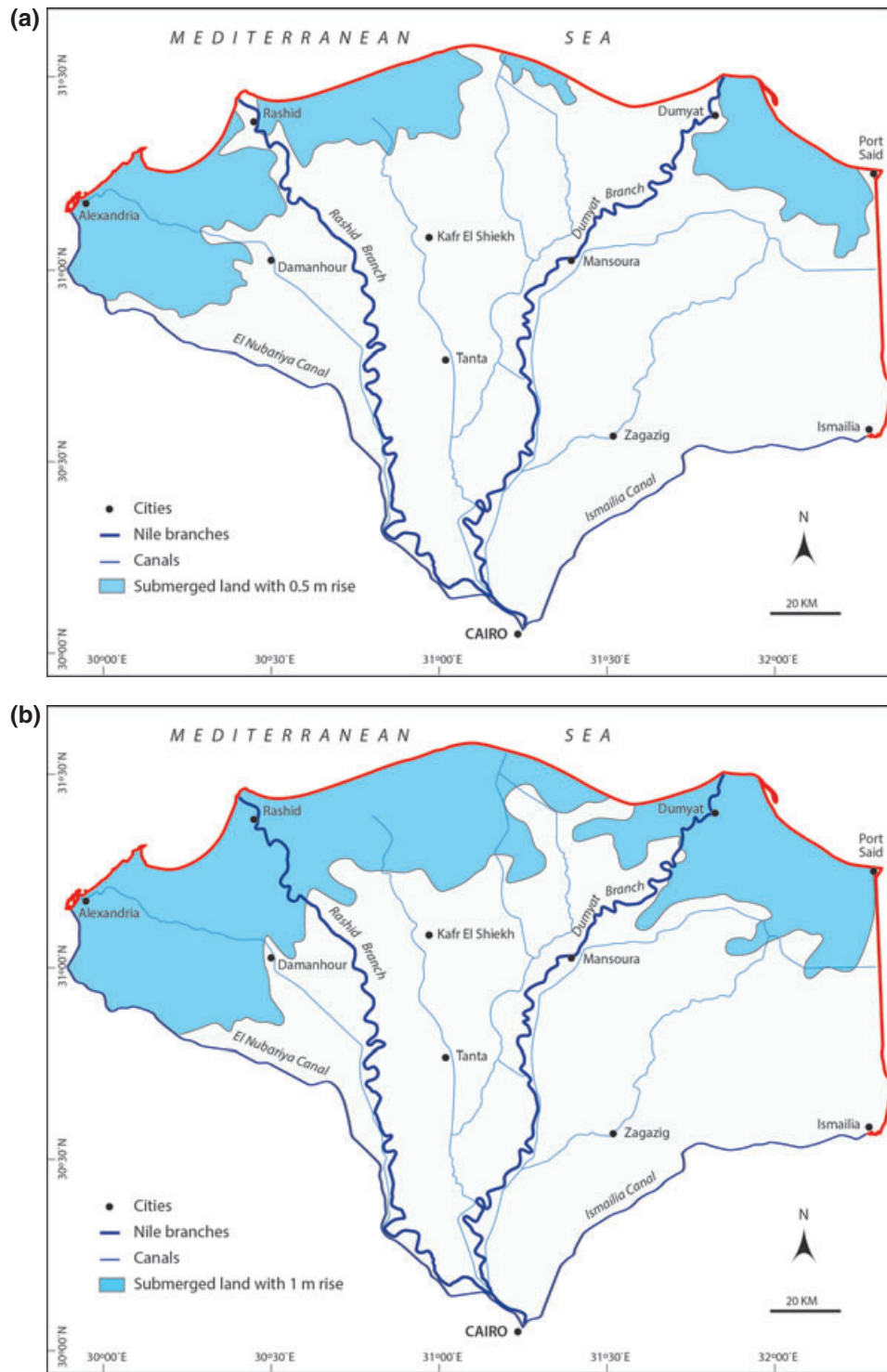
Using the digital elevation models from the Advanced Spaceborne Thermal Emission and Reflection Radiometer, ASTER, (Global DEM) with a special resolution of about 30 m, the shoreline was shifted in the different scenarios to match the seawater level rise of 0.5 and 1.0 m. Due to the flat nature of the topography and the large depression areas in the coastal zone of the Nile Delta Aquifer, the seaside boundary is significantly shifted inland under the condition of seawater rise. The total area of the land of the Nile Delta under the current conditions (0.0 seawater level), as calculated by ARC-GIS is 23,284 km^2.

A land area of 4396 km^2, representing about 19% of the total land of the Nile Delta Aquifer will be lost under the condition of a 0.5 m rise in the Mediterranean seawater level, Figure 4a. On the other hand, 7516 km^2, representing about 32% of the total land will be submerged by the seawater under the condition of a 1.0 m rise of the seawater, Figure 4b. The study domain was modified to reflect the appropriate conditions of seawater level rise and the boundary conditions at the seaside were revised accordingly. In addition, finite element grids were regenerated for the two cases of 0.5 and 1.0 m seawater rise.

The seawater intrusion and the dispersion zone were simulated for the six scenarios listed in Table 2 using calibrated mode. All simulations were conducted under the steady state conditions to reflect the ultimate conditions (worst case) under the suggested seawater rise

Table 2
Climate Change Simulation Scenarios

Scenario	Seawater Level (m)	Pumping (billion m^3/year)
Base scenario (current)	0.0	2.3
One	0.5	1.15
Two	0.5	2.3
Three	0.5	4.6
Four	1.0	1.15
Five	1.0	2.3
Six	1.0	4.6

Figure 4. (a) Submerged land in the coastal zone under the condition of 0.5 m seawater rise. (b) Submerged land in the coastal zone under the condition of 1.0 m seawater rise.

and groundwater pumping. In reality, however, the shift of the shoreline, under the climate change condition, would possibly occur over a period of one century (IPCC 2001, 2007; Cayan et al. 2009). The simulations of the various scenarios reveal that groundwater flow and heads would require few decades to reach the steady state conditions. On the other hand, the solute transport and the dispersion zone would require few centuries to

achieve the steady state conditions. The flow adjusts more rapidly as compared to solute transport and groundwater concentration.

Figure 5a through 5c represents the final status of the seawater intrusion assuming a 0.5 m rise associated with a groundwater pumping of 1.15, 2.3, and 4.6 billion m^3/year, respectively. The results of the current investigation reveal that both Sherif and Singh (1999)
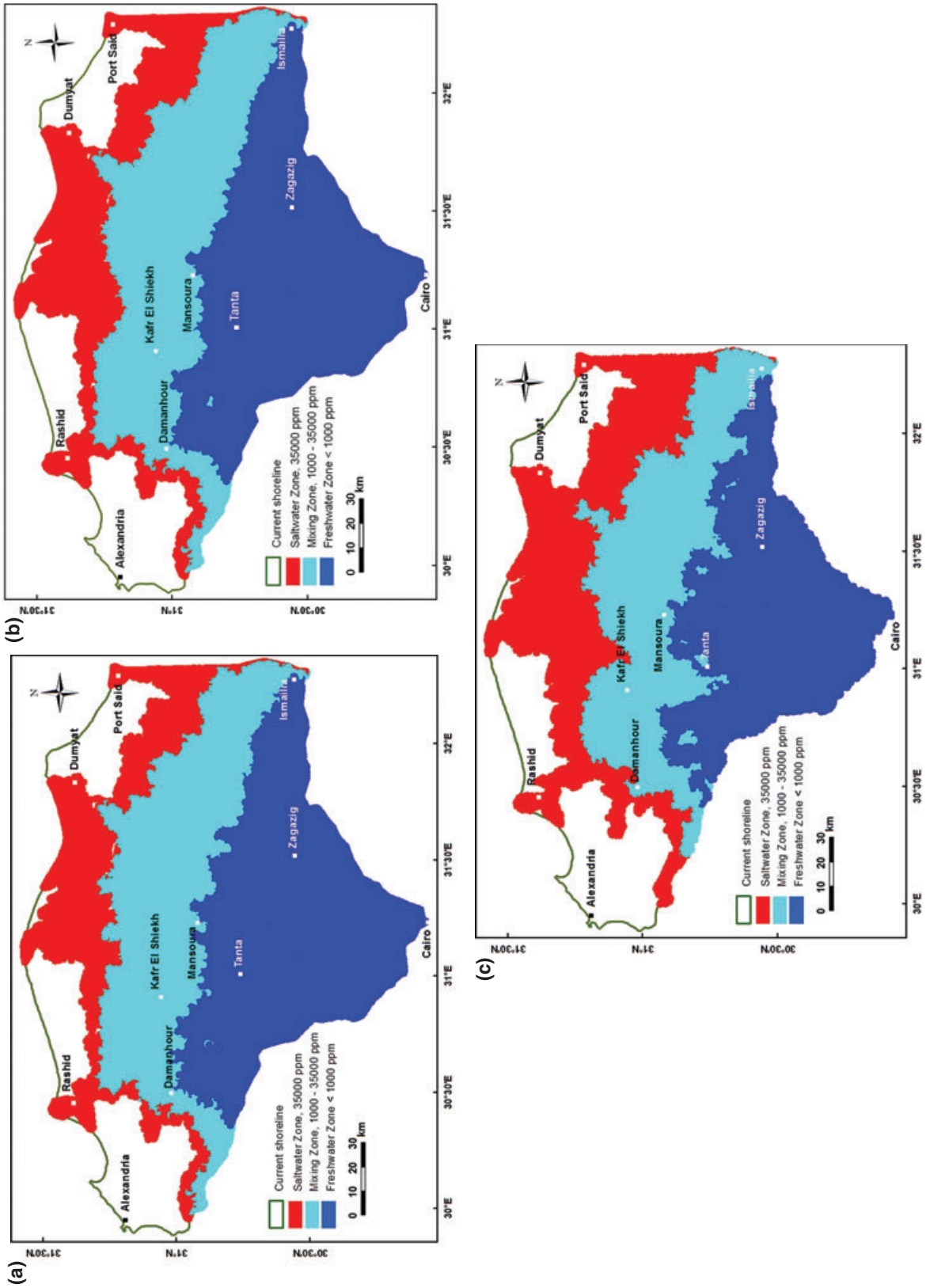
Figure 5. Seawater intrusion under the condition of 0.5 m seawater level rise: (a) scenario one, (b) scenario two, and (c) scenario three.
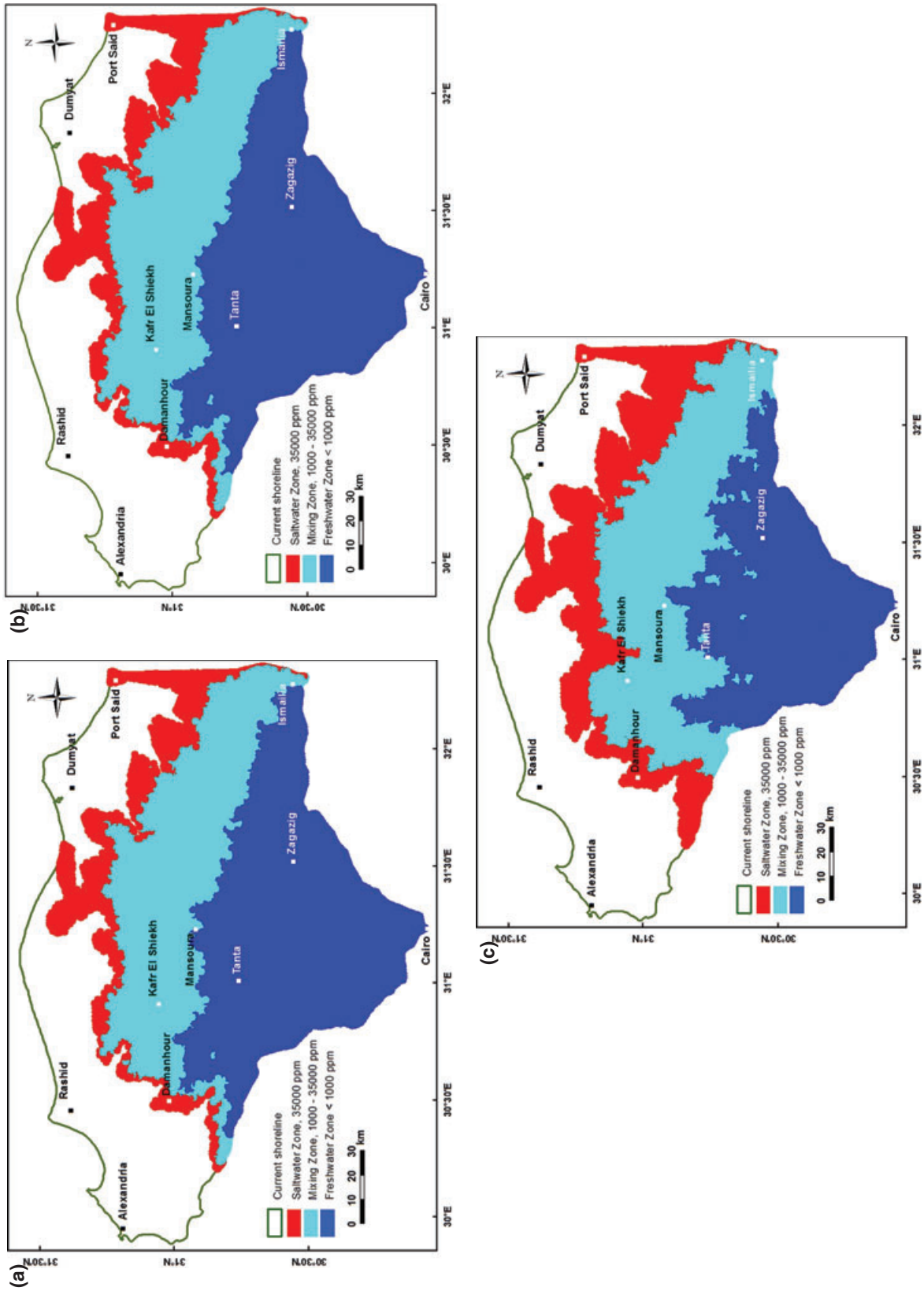
Figure 6. Seawater intrusion under the condition of 1.0 m seawater level rise: (a) scenario four, (b) scenario five, and (c) scenario six.

and Werner and Simmons (2009), underestimated the possible consequences of the seawater rise on the Nile Delta Aquifer due to ignoring the significant landside shift of the seaside boundary.

Figure 6a through 6c represents the final status of the seawater intrusion assuming a 1.0 m rise associated with a groundwater pumping of 1.15, 2.3, and 4.6 billion m^3/year, respectively. Due to the flat nature of the land and the presence of depressions in the coastal zone along with the mild hydraulic gradient of the groundwater table, the seawater level rise and the pumping rates have a significant impact on the groundwater quality in the Nile Delta Aquifer. Scenario six represents the worst case under which the freshwater is encountered in the southern parts of the Nile Delta Aquifer only.

Discussion and Analysis

A very wide dispersion zone is encountered in the Nile Delta Aquifer due to the excessive groundwater pumping form the southern parts of the Delta and also due to the relatively high porosity and permeability of the system. The total volume of the available groundwater in the Nile Delta Aquifer can be estimated from the saturated volume of the porous medium multiplied by the porosity. It should be noted, however, that the aquifer depth, the saturated thickness, and the porosity vary from one point to another and hence the GIS system was employed to calculate the volume of groundwater in the fresh, brackish, and saline zones of the aquifer under the six different scenarios. Table 3 provides estimates for the areas occupied by the three water quality zones and groundwater volumes in the three zones for all tested scenarios using the GIS system.

Under the current conditions (Figure 3b), and considering that the steady state conditions prevail, the total volume of groundwater is estimated at 3459 billion m^3 distributed as 883 billion m^3 of freshwater, 1249 billion m^3 of brackish water with a salinity between 1000 and 35,000 ppm and 1327 billion m^3 of saline water with a salinity of 35,000 ppm, Table 3.

The total volume of available groundwater (fresh, brackish, and saline waters) in the Nile Delta Aquifer will decrease significantly under the condition of seawater level rise as large areas (thousands of km^2) in the coastal zone will be merged to the Mediterranean Sea (Figure 4a and 4b) and the groundwater in such areas will no longer contribute to the groundwater budget in the Nile Delta Aquifer. Using the GIS, the total volumes of groundwater under the conditions of 0.5 and 1.0 m seawater level rise were estimated as 2793 and 2187 billion m^3, respectively, Table 3. More than one-third of the total groundwater volume will be lost under the condition of 1.0 m seawater level rise. However, this water is mostly saline under the current conditions.

Under scenario one, although the groundwater pumping is reduced by 50%, the available freshwater will slightly be reduced from 883 to 860 billion m^3. The volume of saline water in the aquifer will also reduce significantly to about 767 billion m^3 as large volumes will be under the sea and will no longer be considered as an element of the water budget in the aquifer. On the other hand, the volume of brackish groundwater in the transition zone is evaluated as 1166 billion m. Therefore, under this scenario, the loss of total freshwater is not tangible although large lands will be lost. As far as the freshwater is concerned, the 50% reduction in the groundwater pumping has almost balanced the landward shift of the seaside boundary.

Under the two cases of 0.5 (scenarios 1 through 3) and 1.0 m (scenarios 4 through 6) seawater level rise, as the pumping increases, the areas and volumes of the saline water increase and the areas and volumes of freshwater decrease (Table 3). However, the changes in the areas and volumes of the brackish water in the transition zone were relatively small as compared to those of the fresh and saline waters. The volumes of brackish water varied in the range of 1.0 to 1.17 × 10^3 km^3 for the six tested scenarios. On the other hand the volumes of freshwater varied between 513 × 10^3 km^3 for Scenario six to 860 × 10^3 km^3 for Scenario one. Although large coastal lands (19 and 32% of the total area of the Nile Delta) will be submerged under the conditions of 0.5 and 1.0 seawater level rise, the

Table 3
Areas of the Three Water Quality Zones and Groundwater (GW) Volumes in the Three Zones Under Different Scenarios

Scenario	Saltwater Zone Area (10^3 km^2)	Saltwater Zone GW Volume (km^3)	Mixed Zone Area (10^3 km^2)	Mixed Zone GW Volume (km^3)	Freshwater Zone Area (10^3 km^2)	Freshwater Zone GW Volume (km^3)	Total Area (10^3 km^2)	Total GW Volume (km^3)
Basic	7.155	1327	7.311	1249	8.818	883	23,284	3459
One	3.630	767	6.685	1166	8.573	860	18,888	2793
Two	4.294	889	6.369	1099	8.225	804		
Three	5.654	1115	6.280	1037	6.954	641		
Four	1.970	389	5.799	1017	7.998	781	15,768	2187
Five	2.200	431	5.796	1009	7.772	748		
Six	3.564	657	6.298	1018	5.906	513		

actual reduction in the available freshwater volumes will be in the range of 9 and 15% only assuming that the current pumping rates will remain unchanged.

Conclusions

This article presents the first comprehensive assessment for the impacts of the possible water level rise in the Mediterranean Sea on the seawater intrusion in the Nile Delta Aquifer. The problem was investigated under two scenarios of seawater level rise in combination with three scenarios of groundwater pumping. Unlike all previous investigations on the Nile Delta Aquifer, the seaside boundary was revised to account for land submergence and all simulations were conducted in the horizontal views. A comprehensive GIS database was developed and digital elevation models were used to delineate the study domain and the seaside boundary under the conditions of 0.5 and 1.0 m seawater level rise. Currently, the total volume of fresh groundwater in the Nile Delta Aquifer is around 883 km^3.

About 19 and 32% of the total area of the Nile Delta will be submerged under the 0.5 and 1.0 m seawater level rise, respectively. Although about one-third of the groundwater resources will be lost under the condition of 1.0 m seawater rise, the available volume of the freshwater will be reduced by about 15% assuming that the current pumping rates will be maintained. Reducing the groundwater pumping by 50% would mostly sustain the freshwater resources under the condition of 0.5 m seawater level rise.

Acknowledgments

References

Bear, J., A. Cheng, S. Sorek, D. Ouazar, and I. Herrera. 1999. *Seawater Intrusion in Coastal Aquifers Concepts, Methods and Practices*. Theory and Applications of Transport in Porous Media, Vol. 14, 640.

Brown, S., A.S. Kebede, and R.J. Nicholls. 2011. Sea-level rise and impacts in Africa, 2000–2100. Southampton, United Kingdom: School of Civil Engineering and Environment, University of Southampton. Internal report.

Cayan, D., M. Tyree, M. Dettinger, H. Hidalgo, T. das, E. Maurer, P. Bromirski, N. Graham, and R. Flick. 2009. Climate change scenarios and sea level rise estimates for California 2008 climate change scenarios assessment. California Climate Change Center. CEC-500-2009-014-F.

Coutellier, V., and D.J. Stanley. 1987. Late Quaternary stratigraphy and paleogeography of the eastern Nile delta shelf. *Marine Geology* 77: 257–275.

Dahab, K.A. 1993. Hydrogeological evolution of the Nile delta after the High Dam construction. PhD thesis, Menofia University, Egypt.

Diersch, H.J.G. 2006. FEFLOW manual. 190. Berlin: WASY GmbH. www.wasy.de.

Diersch, H.J.G. 2002. WASY Software – FEFOW: Finite Element Subsurface Flow & Transport Simulation System: Reference Manual. WASY Institute for Water Resources Planning and Systems Research Ltd., 2002, 292.

Diersch, H.J.G., and O. Kolditz. 1998. Coupled groundwater flow and transport: 2. Thermohaline and 3D convection systems. *Advances in Water Resources* 21: 401–425.

El-Sadek, A., M. El Kahloun, and P. Meire. 2008. Ecohydrology for integrated water resources management in the Nile Basin. *Ecohydrology and Hydrobiology* 8, no. 2–4: 77–84.

Galeati, G., G. Gambolati, and S.P. Neumann. 1992. Coupled and partially coupled Eularian-Langangrian model of freshwater-seawater mixing. *Water Resource Research* 28: 149–165.

Henry, H.R. 1964. Effects of dispersion on salt encroachment in coastal aquifers. Sea Water in Coastal Aquifers, U.S. Geol. Surv. Supply Pap., 1613-C, C71–C84.

Hurst, H.E. 1952. *The Nile*, London, 326.

Intergovernmental Panel of Climate Change (IPCC). 2007. Climate change 2007: Impacts, adaptations, and vulnerability. Contribution of Working Group II to the fourth assessment report of the Intergovernmental Panel on Climate Change. Cambridge, UK: Cambridge University Press.

Intergovernmental Panel of Climate Change (IPCC). 2001. Climate change 2001: Impacts, adaptations, and vulnerability. Contribution of Working Group II to the third assessment report of the Intergovernmental Panel on Climate Change. Cambridge, UK, and New York: Cambridge University Press.

Kacimov, A.R., and M.M. Sherif. 2006. Sharp interface, one-dimensional seawater intrusion into a confined aquifer with controlled pumping: Analytical solution. *Water Resources Research* 42, no. 6: W06501.

Kacimov, A.R., M.M. Sherif, J.S. Perret, and A. Al-Mushikhi. 2009. Control of sea-water intrusion by salt-water pumping: Coast of Oman. *Hydrogeology Journal* 17, no. 3: 541–558. DOI:10.1007/s10040-008-0425-8

Kashef, A.I. 1983. Salt water intrusion in the Nile Delta. *Ground Water* 21, no. 2: 160–167.

Kashef, A.I. 1981a. The Nile-one River and nine countries. *Journal of Hydrology*: 53–71.

Kashef, A.I. 1981b. Technical and ecological impacts of the High Aswan Dam. *Journal of Hydrology*: 73–84.

Kinzelbach, W. 1986. *Groundwater Modeling*. New York: Elsevier.

Klotz, D. 1973. Untersuchunger zur dispersion in porosen medien. *Zeitschrift der Deutschen Geologischen Gesellschaft* 124: 523–533.

Langevin, C.D, and A.M. Dausman. 2005. Numerical simulation of saltwater intrusion in response to sea level rise, impacts of global climate change. In *Proceedings of World Water and Environmental Resources Congress 2005, ASCE Conf. Proc*. DOI: 10.1061/40792(173)376

Lee, C.H., and R.T.-Sh Cheng. 1974. On seawater encroachment in coastal aquifers. *Water Resources Research* 10, no. 5: 1039–1043.

Lenda, A., and A. Zuber. 1970. Tracer dispersion in groundwater experiments. *Isotope Hydrology*, IAEA-SM, 137, 129–134.

Mikhailova, M. 2001. Hydrological regime of the Nile Delta and dynamics of its coastline. *Water Resources* 28, no. 5: 477–490.

Oude Essink, G.H.P. 1996. Impact of sea level rise on groundwater flow regimes. A sensitivity analysis for the Netherlands. 428. Ph.D. thesis, Delft University of Technology, Delft, Delft Studies in Integrated Water Management 7.

Pinder, G.F., and H.H. Cooper Jr. 1970. A numerical technique for calculating the transient position of the saltwater front. *Water Resources Research* 9: 1657–1669.

Post, V., and E. Abarca 2010. Preface: Saltwater and freshwater interactions in coastal aquifers. *Hydrogeology Journal* 18: 1–4.

Rahmstorf, S., A. Cazenave, J.A. Church, J.E. Hansen, R.F. Kelling, D.E. Parker, and R.C.J. Somerville. 2007. Recent climate observations compared to projections. *Science* 316, no. 5825: 709.

RIGW/IWACO. 1990. Development and management of groundwater resources in the Nile Valley and Delta: Assessment of groundwater pollution from agricultural activities, Internal report, Research Institute for Groundwater, El Kanater El Khairia, Egypt.

Said, R. 1962. *The Geology of Egypt*. Amsterdam, The Netherlands: Elsevier.

Said, R. 1993. *The Nile River: Geology, Hydrology, and Utilization*. New York: Pergamon.

Sanford, W.E., and J.P. Pope. 2010. Current challenges using models to forecast seawater intrusion: lessons from the Eastern Shore of Virginia, USA. *Hydrogeology Journal* 18: 73–93. DOI:10.1007/s10040-009-0513-4

Segol, G., and G.F. Pinder. 1976. Transient simulation of saltwater intrusion in southeastern Florida. *Water Resources Research* 12: 65–70.

Sherif, M.M. 1999. The Nile Delta aquifer in Egypt. In *Seawater Intrusion in Coastal Aquifers: Concepts, Methods and Practices*, ed. Bear et al., vol. 14: *Theory and Application of Transport in Porous Media*, 559–590. The Netherlands: Kluwer Academic Publishers.

Sherif, M.M., and V.P. Singh. 1999. Effect of climate changes on seawater intrusion in coastal aquifers. *Hydrological Processes* 13, no. 8: 1277–1287. DOI:10.1002/(SICI)1099-1085 (19990615) 13:8<1277

Sherif, M.M., A. Sefelnasr, and A. Javadi. 2012. Incorporating the concept of equivalent freshwater head in successive horizontal simulations of seawater intrusion in the Nile Delta Aquifer, Egypt. *Journal of Hydrology* 464–465: 186–198. DOI:org/10.1016/ j.jhydrol.2012.07.007

Sherif, M.M., V.P. Singh, and A.M. Amer. 1988. A two dimensional finite element model for dispersion (2D-FED) in coastal aquifers. *Journal of Hydrology* 103: 11–36.

Sherif, M.M., V.P. Singh, and A.M. Amer 1990. A sensitivity analysis of "2D-FED," a model for seawater encroachment in leaky coastal aquifers. *Journal of Hydrology* 118: 343–356.

Simpson, M.J., and T.P. Clement. 2004. Improving the worthiness of the Henry problem as a benchmark for density dependent groundwater flow models. *Water Resources Research* 40: W01504. DOI:10.1029/2003WR002199

Voss, C.I. 1984. SUTRA: A finite-element simulation model for saturated-unsaturated fluid-density-dependent groundwater flow with energy transport or chemically-reactive single-species solute transport. U.S. Geological Survey Water Resources Investigation Report 84-4369.

Werner, A.D., and C.T. Simmons. 2009. Impact of sea-level rise on seawater intrusion in coastal aquifers. *Ground Water* 47, no. 2: 197–204. DOI:10.1111/j.1745-6584.2008.00535.x

Yechieli, Y., E. Shalev, S. Wollman, Y. Kiro, and U. Kafri. 2010. Response of the Mediterranean and Dead Sea coastal aquifers to sea level variations. *Water Resources Research* 46: W12550. DOI:10.1029/2009WR008708